

Evaluation of Communication Requirements for Voltage Regulation Control with Advanced Inverters

Matthew J. Reno, Jimmy E. Quiroz, Olga Lavrova, Raymond H. Byrne
Photovoltaics and Distributed Systems Integration; Data Analysis and Exploitation
Sandia National Laboratories
Albuquerque, USA

Abstract—A central control algorithm was developed to utilize photovoltaic system advanced inverter functions, specifically fixed power factor and constant reactive power, to provide distribution system voltage regulation and to mitigate voltage regulator tap operations by using voltage measurements at the regulator. As with any centralized control strategy, the capabilities of the control require a reliable and fast communication infrastructure. These communication requirements were evaluated by varying the interval at which the controller sends dispatch commands and evaluating the effectiveness to mitigate tap operations. The control strategy was demonstrated to perform well for communication intervals faster than the delay on the voltage regulator (30 seconds). The communication reliability, latency, and bandwidth requirements were also evaluated.

Keywords—automatic generation control; centralized control; communication networks; photovoltaic systems; reactive power

I. INTRODUCTION

With increasing penetrations of distributed PV being interconnected with the grid, there is increased attention focusing on the ability to control the distributed energy resources (DER) and leverage the advanced inverter capabilities of the solar inverters. Specifically, the reactive power output of the inverter can be controlled using local advanced inverter functions, such as volt-VAr, to mitigate voltage violations [1] and voltage variations [2]. Studies have shown how these local volt-VAr functions can improve the grid performance and can be particularly effective at increasing the PV hosting capacity of a distribution system [3, 4].

With faster and more easily accessible communication through recommendations such as the California Rule 21 [5], a centralized controller can communicate and control all PV inverters on a feeder in a more optimal way than the autonomous local control. In [6-9], a reactive power control strategy is proposed to dispatch solar inverters to minimize losses while keeping the voltage within allowable ranges. In [10], the tradeoff between optimal control and fair control of PV inverters is discussed. Centralized control of advanced inverters can include communication and control of other voltage regulation devices on the feeder to minimize interactions and improve the overall voltage [11]. Centralized control strategies can also be used in conjunction with local volt-VAr control to continually optimize and improve the state of the system [12] for purposes such as voltage imbalance [13].

While coordinated (e.g. centralized, distributed, hierarchical, etc.) control can provide more optimal solutions

than local reactive power control in the inverters, the effectiveness of the control requires a reliable and fast communication infrastructure. The focus of this work was to evaluate the potential communication requirements when utilizing advanced inverter functions from a distribution perspective. The specific use case presented in this paper is to use centralized control of PV reactive power to mitigate PV-induced voltage regulator (VREG) tap operations.

Voltage regulator tap operations were studied due to their shorter temporal urgency when compared to other steady-state impact requirements. Most voltage and thermal standards and limitations occur on the order of 10-minute averages or greater, whereas, voltage regulator control delay settings are usually on the order of 30-60 seconds. The concern for voltage regulation devices is that a significant increase in the number of device operations could result in accelerated degradation and/or the need for a more aggressive maintenance schedule [14].

The objective of the research was to simulate the dispatch of control signals to the PV systems on a feeder to decrease the number of tap changes and wear on the regulator. The effectiveness of the controller depended on how quickly it could respond to system changes, such as quick ramps in PV output. The necessary communication infrastructure was tested by varying the communication interval, i.e. how often the controller obtains necessary parameters from inverters, calculates new settings, and dispatches them. The advanced inverter functions used to mitigate tap changes were fixed power factor (PF) (INV3) and constant reactive power (VAr) (VV13) [15].

II. TEST SETUP

A rural 12kV distribution feeder in southern California was chosen as the test feeder. The feeder consists of 2970 medium- and low-voltage buses and 2569 lines servicing 1447 customers through 401 service transformers. A map showing the layout of the feeder topology and the existing voltage regulation devices is shown in Figure 1. There is a line VREG bank (three single-phase VREGs) on the feeder backbone about 6 km from the substation and five switching capacitors. The VREG uses a sequential control [16] with cogeneration mode under reverse power flow of the VREGs. The feeder has a peak load of 6.41 MW and a minimum load of 1.29 MW.

The purpose of the VREG (marked in red in Figure 1) is to regulate the downstream voltage. The three single-phase VREGs each measure the voltage on the secondary winding of the transformer, and mechanically switch taps to buck or boost

the downstream voltage. The VREG control includes a voltage setting, a voltage bandwidth, and a time delay setting. If the voltage deviates outside the voltage setpoint plus or minus half the bandwidth for more than the delay time, a tap change occurs. The time delay for these VREGs is 30 seconds.

The peak load week of June 27th to July 3rd was selected as the simulation week for all studies. The measured substation supervisory control and data acquisition (SCADA) data at 1-minute resolution was used to model the load variation. Quasi-static time series (QSTS) power flow analysis [14] was performed at 1-second resolution by linearly interpolating the load data to 1-second resolution. The analysis was performed in OpenDSS using the GridPV toolbox [17]. In order to speed up the QSTS analysis, the feeder model was reduced to a smaller equivalent model [18].

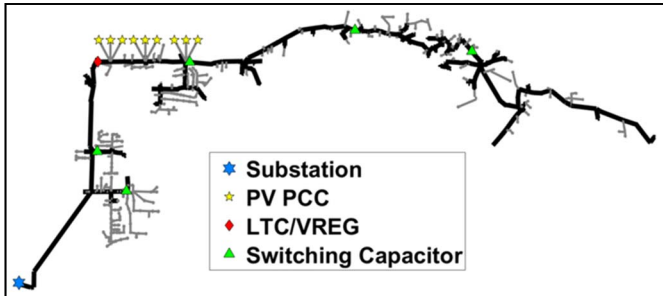


Figure 1. Map of the test feeder with the PV test scenario.

A total of 9 PV systems were simulated at three locations just downstream of the VREGs, each consisting of a system from all three-phases, as shown by the yellow stars in Figure 1. A very high penetration of PV was required to significantly increase the number of tap changes on the VREGs. Each PV system was set to 311 kW, 3 per phase, yielding an aggregate total of 2.8 MW of PV. The penetration was 80% of the load downstream of the VREG and 45% of the total feeder load. The penetration was 46.3% of the normal conductor thermal capacity downstream of the VREG.

The irradiance profile for each location was generated using 1-second resolution measurements from San Diego, California. The measured irradiance was time-shifted based on the distance between each transformer, assuming clouds propagate from west to east and the maximum speed of 24 m/s from a year of cloud speeds at the feeder location. For each transformer, the time-shifted measured irradiance was converted to latitude-tilt (of the feeder location) plane-of-array (POA) irradiance using the Erbs decomposition and Hay/Davies transposition models [19]. The Sandia Array Performance Model [20] and Sandia Inverter models [21] were used to obtain PV power output from the POA irradiance. By using estimated outputs for smaller systems and using the fastest cloud speed, the worst case scenario for solar variability with underestimated geographical smoothing was simulated.

Figure 2 shows the basecase (no PV) and unity PF PV case feeder-level and VREG-level real power profiles for the simulation week. The number of tap changes in these cases was used as the metrics of success of the controller simulations.

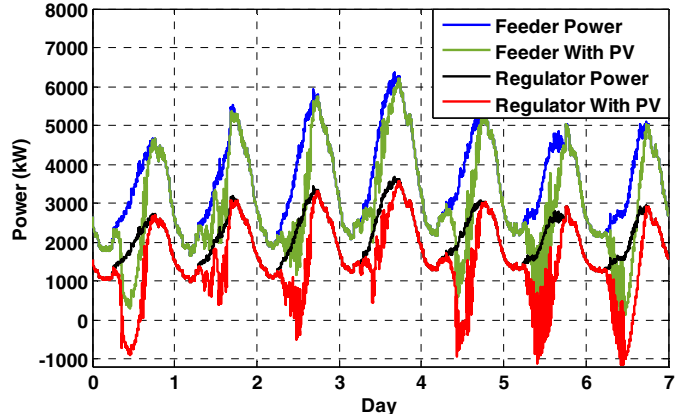


Figure 2. Feeder and voltage regulator real power during the simulation week for the basecase and the unity power factor PV case.

III. CENTRALIZED CONTROLLER LOGIC

It was assumed that the central controller receives measurements from the voltage regulator and the PV systems and could send dispatch control signals back to the PV systems. Depending on the utility, it is commonly standard practice to require utility communication and potentially control of large systems, even sometimes as low as 100 kW. The initial testing assumed that the controller requested and obtained parameters from all PV systems, processed calculation of dispatch values, dispatched values, and inverters implemented dispatched commands all within a second of the communication interval. These assumptions about the communication infrastructure are considered later in the paper to investigate their impact. It is also assumed that an accurate distribution power flow model is available for the controller to derive the relationship between PV reactive power injections and the voltage at the VREG.

Figure 3 illustrates the logic of the voltage regulation controller using advanced inverters. The overall concept of the control was to use the voltage measurements at the VREG to modify the reactive power output of the solar inverters to keep the voltage consistent at the VREG. This provides voltage regulation for the feeder using existing measurements, and it also has the benefit of reducing the VREG tap changes that cause wear and tear on the device.

It was assumed that the VREG is not modified or externally-controllable in any way, therefore the controller settings were based on the VREG's voltage setpoint and voltage bandwidth settings. The centralized controller used a similar strategy as a VREG where new settings are dispatched to the PV inverters only if the voltage is outside the deadband. The controller compared the measured voltage of each phase to the known VREG settings to determine if the voltage is out of band. If no phases are out of band, no action is taken. To avoid excessive activity right along the VREG deadband edges, the controller implemented an adjustable tighter deadband, set to 80% of the width of the VREG deadband.

If the voltage was outside the deadband, the amount the voltage is out of band was calculated. This $\Delta V_{ctrlEdge}$ value was calculated as simply the difference between each phase measured voltage to the edge of the controller deadband (either

top or bottom). The $\Delta V_{\text{CtrlEdge}}$ was multiplied by an adjustable gain factor (F_G), set to 2, to bring the voltage inside the band proportional to $\Delta V_{\text{CtrlEdge}}$. The resulting scaled ΔV was limited by a saturation block to keep it from going beyond the controller deadband midpoint.

The amount of reactive power change (ΔQ) necessary to move the voltage back into the deadband (ΔV) was calculated based on voltage sensitivities [22]. The voltage sensitivities were determined using iterative, load-flow solutions to find the change in voltage at bus i due to a reactive power injection at bus j , with units of $V_{\text{pu}}/\text{kVAr}$. With multiple injection points (j) affecting the voltage at multiple buses (i), an SQ matrix of voltage sensitivities was determined, with each element of the matrix determined using (1)

$$SQ_{ij} = \frac{\Delta V_i}{\Delta Q_j} \quad (1)$$

The SQ matrix was fixed and does not change. For this analysis SQ was formed by simulating the voltage change at each voltage regulator due to each PV reactive power injection. The VArS of each phases' PV system at each of the three locations was varied from 0 to 311 kVAr (full rated VAr output), and the changes in all three phases of voltage at the VREG were recorded, resulting in the 3x3 SQ matrix in (2). The ΔQ s were calculated using (3) with the SQ matrix and the measured ΔV .

$$[SQ] = \begin{bmatrix} 7.17E - 05 & 1.37E - 06 & -2.01E - 05 \\ -2.07E - 05 & 7.35E - 05 & 1.41E - 06 \\ 1.10E - 06 & -2.00E - 05 & 7.24E - 05 \end{bmatrix} \quad (2)$$

$$[\Delta Q] = [SQ]^{-1} * [\Delta V] \quad (3)$$

Note that the ΔV was calculated from the per phase voltage differences between present VREG voltages and the pertinent controller deadband edge. The SQ matrix was also calculated using the full 3-phase unbalanced calculation to determine the interaction between phases. Since all phases are sensitive to any single-phase VAr change, the controller processed values for all phases even if just one phase is out of the deadband, and the ΔQ s are all calculated simultaneously.

During the daytime, the ΔQ s values were directly dispatched to the PV inverters to modify their reactive power to the new setting. The night or daytime decision block could be determined by many different settings (time of day, irradiance measurement, inverter real power output, etc.). In these simulations, daytime was defined by a PV real power output greater than 5% of its rated power. The purpose of this section of the control was to be able to accommodate many inverters that normally turn off below a certain power output threshold due to efficiencies and to conserve power.

During the nighttime, a control flag was incorporated to allow activation of the controller at night. If night control was not enabled, the PV inverters would be off and not injecting real or reactive power. For the following simulation results, the night control was always enabled, and the inverters continued to be dispatched during the nighttime to demonstrate the full potential inverters have for voltage regulation. Dispatching during only daylight hours resulted in the controller mitigating all tap changes during the day, either

caused by PV variability or diurnal load variation, but the voltage regulator changed taps to regulate the voltage at night.

Finally, given the popularity of the fixed power factor capabilities of PV inverters, the fixed power factor (INV3) dispatch was compared in addition to the constant reactive power (VV13) [15]. Figure 3 shows the control diagram for the VV13 dispatch, but INV3 dispatch would look similar with only the daytime block being modified to "Dispatch phase Power Factors" instead of "Dispatch phase ΔQ s". For the PF-based controller during the day, the per-phase PFs were calculated with (4) by summing all the PV real and reactive power outputs of the phase with the phase ΔQ (A-phase used for example): If night dispatch was allowed, since no real power was being generated, the night controller would continue to dispatch constant reactive power (VV13).

$$PF = \frac{\sum P_A}{\sqrt{(\sum P_A)^2 + ((\sum Q_A) + \Delta Q_A)^2}} \quad (4)$$

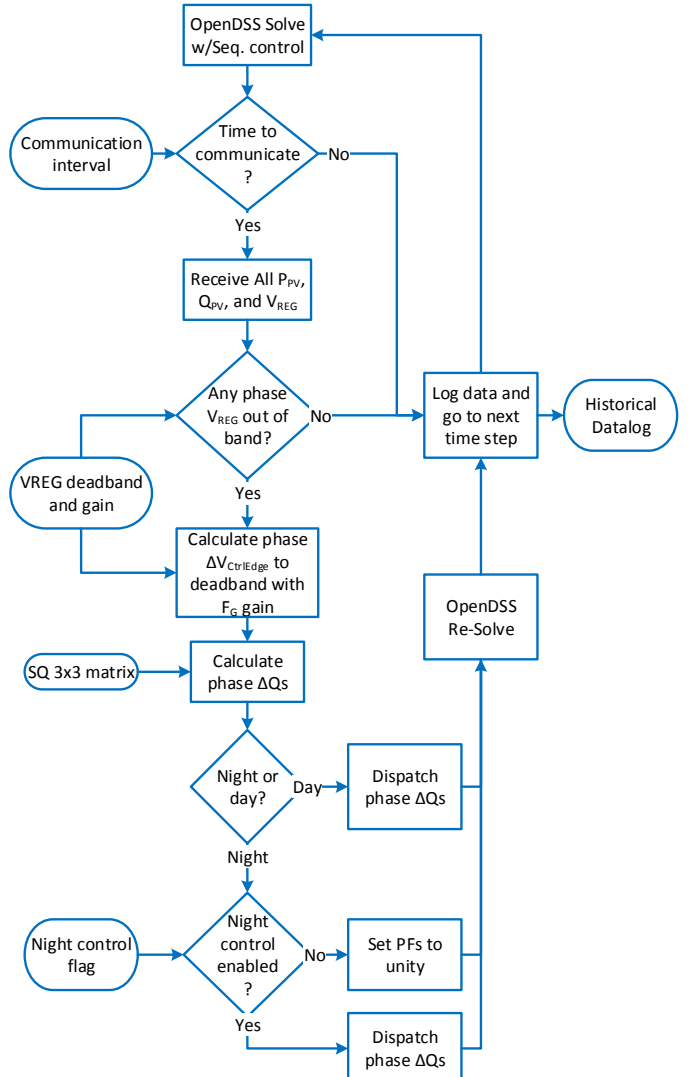


Figure 3. Controller diagram for voltage regulation using advanced inverter VAr (VV13).

IV. VOLTAGE REGULATION CONTROLLER RESULTS

A. Power Factor Dispatch Results

The controller and varying control intervals were implemented in MATLAB. First, the PF-based controller, that dispatches fixed power factor settings to the inverters, was evaluated due to the popularity of the INV3 advanced inverter function. The results of the PF-based controller simulations illustrated a valuable discovery about the stability of the control algorithm. Because the PV real power (kW) varies with irradiance, the PV real power output is highly variable and can produce large, quick ramps in output. With a fixed PF dispatch, these ramps also create large ramps in reactive power, which can be especially problematic when using the high level of variability defined for these studies.

Since distribution system X/R ratios are generally greater than 1, the large, quick ramps in reactive power output create a larger impact on the voltage compared to solely changing the real power output, which increases the voltage flicker. The power factor dispatched to the PV systems was appropriate for that instant, but once the real power changes, the impact on the VArS became more detrimental than helpful. When the communication interval was short enough, these large swings in reactive power output could be quickly compensated by dispatching new power factors. For example, with 1-second communication update interval and no communication delays, the controller worked perfectly removing all regulator tap changes. As the communication interval was increased, the fixed PF caused amplified voltage swings on the feeder, which conflicted with the VREG and caused thousands of tap changes.

B. Reactive Power Dispatch Results

Second, the VAr-based controller was developed and evaluated. This controller had the advantage that any quick ramps in solar irradiance did not change the reactive power output. For high solar variability, this controller proved to be more effective with stable reactive power flows on the feeder. The results for the simulation week are shown in Figure 4 compared to the basecase simulation with unity power factor PV. In the top part of the figure, the solar variability created a large number of tap changes at unity power factor, but all tap changes were completely removed by the centralized dispatch of PV reactive power. The middle part of Figure 4 shows the reactive power injection from a single PV inverter. The bottom of Figure 4 shows the voltage at the VREG. The black dashed lines are the voltage bandwidth limits that the VREG is trying to maintain. While there are temporary voltage excursions, the controller provided voltage regulation fast enough to keep the voltage at the VREG within the voltage bandwidth without it having to change taps.

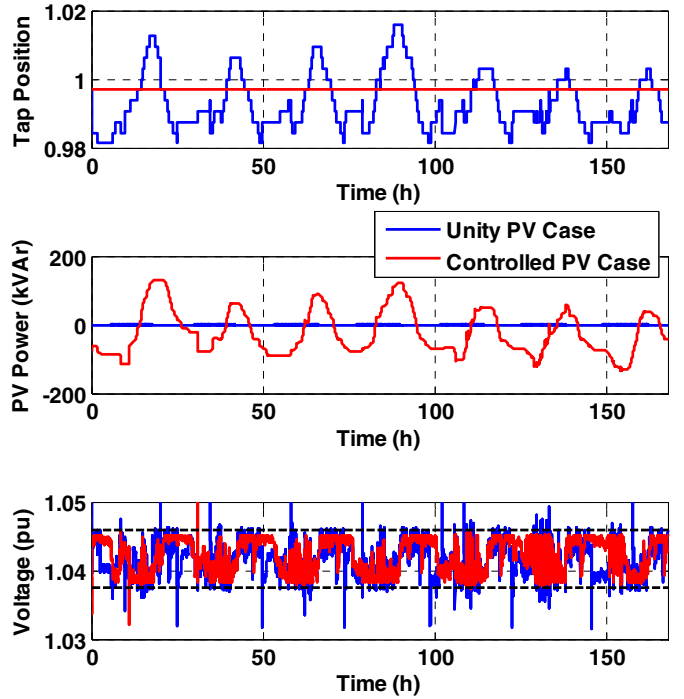


Figure 4. VAr based controller results for the simulation week with 1-second communication intervals.

V. COMMUNICATION RESULTS

In the previous section, the VAr-based controller was demonstrated to mitigate all VREG tap changes with fast and reliable communication. The communication infrastructure requirements were tested by investigating four components of the communication network: communication interval, reliability, latencies, and bandwidth. The sections below demonstrate how the effectiveness of the voltage regulation control is dependent on the communication network by quantifying the impact to the number of voltage regulator tap changes.

A. Communication Interval Results

The communication interval, i.e. how frequently communication must occur, was studied by varying the communication between the inverters and controller from every second to every 5 minutes. As data and command signals were exchanged less often, the effectiveness of the controller decreased. Figure 5 shows the results for different communication intervals during the simulation week for the VAr-based controller simulations with night control enabled for 100% reliable communication, no network delays, and enough bandwidth to communicate with every PV system simultaneously.

For all intervals less than the VREG delay of 30 seconds, the controller mitigated all VREG tap operations by modifying the PV reactive power to keep the voltage within the deadband. At communication intervals longer than 30 seconds, only voltage deviations that occurred between communication intervals required a VREG tap operation. In this case, even a 5-minute communication interval would be considered successful since it is still below the basecase and unity PF case levels.

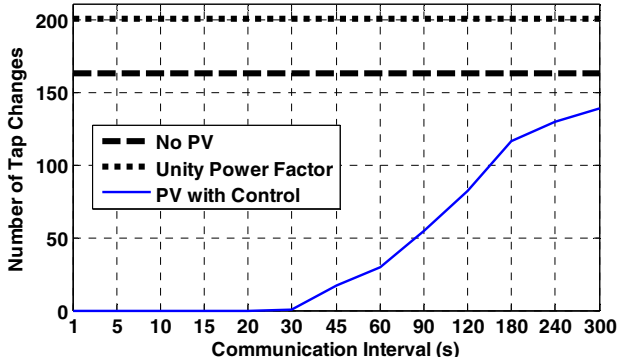


Figure 5. VAr based controller results for the simulation week with different controller communication intervals

B. Communication Reliability Results

The communication reliability was tested by implementing a random probability of successful communication. For example, when simulating a system with 99% reliability, each communication signal had a 99% probability of being received without errors. This stochastic model was applied to both the measurement signal coming into the controller and the dispatch signal going to the inverters. Due to the stochastic nature of the simulation, a given communication failure could occur during times the voltage was within band and did not cause problems, or the communication failure could result in a voltage issues being missed with the VREG having to change taps. The QSTS simulation was run twice for each test condition so that the results could be averaged. The results in Figure 6 show an extreme sweep of different communication network reliabilities for a few communication intervals.

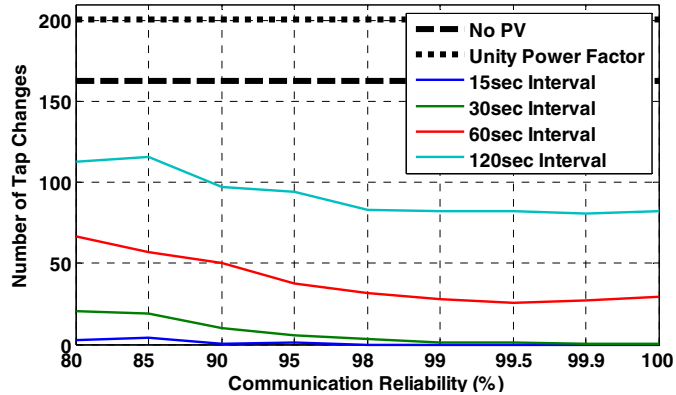


Figure 6. Controller results for different communication intervals and network reliability.

C. Communication Latency Results

In the previous simulations, it was assumed that there were no communication latencies and the time from measurement to implementing the new setting was within the 1-second simulation timestep. In reality, there are many communication delays. For example, depending on the sensor, advanced inverters can take almost 0.5 seconds to measure and process the system voltage [23]. For some types of communication, especially if there are third parties involved, the communication could take up to a second to be received by the controller. The controller will have to wait for all measurement signals, process the data, and then retransmit the

new dispatch settings. Finally, the inverter may take up to a second to reach its new setpoint [23]. While this would generally be achieved in a few seconds, the effect of the communication latencies was tested by increasing the delay up to 20 seconds from the time of measurement to implementation of the settings. Figure 7 shows the number of VREG tap changes during the simulation week for different communication intervals and communication delays.

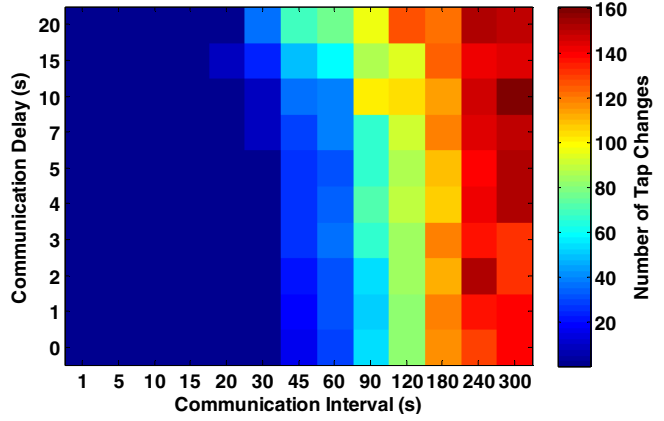


Figure 7. Number of tap changes during the simulation week with different communication intervals and network delays.

D. Communication Bandwidth Results

Finally, some communication networks could be constrained by the available bandwidth. This is especially true for power line carrier (PLC) communication or in high PV penetration scenarios with thousands of PV systems. In these situations, the controller may not be able to communicate with all PV inverters at the same time, so a rotating control was developed to control part of the PV systems at a time. Figure 8 shows the results when communicating with a third of the PV systems at a time. In order to perform the control actions, the controller still had to receive the voltage at the VREG each time, but only communicated (measurements and dispatch) with a third of the PV inverters. The rotating type control performed better than slower communication intervals (e.g. communicating with a third of the systems every 30 seconds was better than communicating with all systems every 90 seconds), but the effect of bandwidth-limited communications systems is seen by the higher red line in Figure 8.

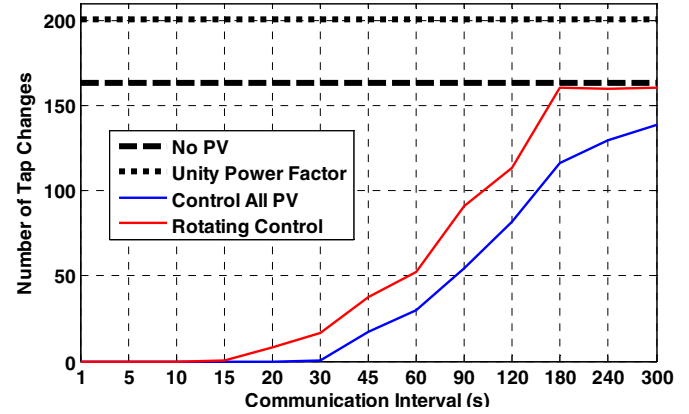


Figure 8. Bandwidth-limited control that could only rotate through communicating with a third of the PV systems at a time.

VI. CONCLUSIONS AND FUTURE WORK

A central control algorithm was developed to utilize photovoltaic system advanced inverter functions, specifically fixed power factor and constant reactive power, to provide distribution system voltage regulation and to mitigate voltage regulator tap operations by using voltage measurements at the regulator. The controller was developed to work for central or distributed (unbalanced) PV on an actual 3-phase distribution system. The necessary communication infrastructure for effective control was evaluated by testing four different communication aspects: 1) interval, 2) reliability, 3) latency, and 4) bandwidth.

The tap operation results of the different communication interval settings were compared to the feeder basecase and unity power factor tap operation totals for a week-long QSTS simulation performed at one-second resolution. The power factor based dispatch introduced complications under variable output conditions. The constant reactive power based control performed well, mitigating all tap changes up to 30 seconds and remaining below the basecase and unity power factor thresholds up to 300 second communication intervals. These conclusions matched other similar research that showed energy storage systems required 15-second communication intervals to mitigate solar variability on the distributed PV system [24].

The reliability of the communication network did not have a noticeable impact on the effectiveness of the controller as long as it was at least 98% reliable. For the communication latencies, delays of 10 seconds or greater had a noticeable impact on the system controller. Finally, it was shown that for bandwidth-limited communication networks, a rotating control improved the results from communicating less frequently.

For initial tests and focus on functionality of the control algorithms, the inverters in the model were designated with an AC-to-DC ratio of 1.2, which could always provide significant reactive power support even at full real power output. Experiments will be conducted with a reduced ratio that will limit the amount of VAr support the inverters could provide and possibly result in the need for more tap operations from the VREG to regulate voltage. Since the control algorithm was solely focused on the goal of tap operation reductions, other important impacts such as thermal limitations, ANSI voltage compliance [25], and increased losses were not monitored. These aspects will be added as limiting factors to the control algorithm as well.

REFERENCES

- [1] M. J. Reno, R. J. Broderick, and S. Grijalva, "Smart Inverter Capabilities for Mitigating Over-Voltage on Distribution Systems with High Penetrations of PV," in *IEEE Photovoltaic Specialists Conference*, Tampa, FL, 2013.
- [2] R. Aghatehrani and A. Golnas, "Reactive power control of photovoltaic systems based on the voltage sensitivity analysis," in *IEEE Power and Energy Society General Meeting*, 2012.
- [3] T. Stetz, F. Marten, and M. Braun, "Improved Low Voltage Grid-Integration of Photovoltaic Systems in Germany," *IEEE Transactions on Sustainable Energy*, vol. 4, 2013.
- [4] J. Seuss, M. J. Reno, R. J. Broderick, and S. Grijalva, "Improving Distribution Network PV Hosting Capacity via Smart Inverter Reactive Power Support," in *IEEE PES General Meeting*, Denver, CO, 2015.
- [5] California Energy Commission (CEC) & California Public Utilities Commission (CPUC), Smart Inverter Working Group Phase 2 Recommendations, Recommendations for Utility Communications with Distributed Energy Resources (DER) Systems with Smart Inverters, Draft v9, February 2015
- [6] M. Farivar, R. Neal, C. Clarke, and S. Low, "Optimal inverter VAR control in distribution systems with high PV penetration," in *IEEE PES General Meeting*, 2012.
- [7] H. G. Yeh, D. F. Gayme, and S. H. Low, "Adaptive VAR Control for Distribution Circuits With Photovoltaic Generators," *IEEE Transactions on Power Systems*, vol. 27, pp. 1656-1663, 2012.
- [8] Z. Shen and M. E. Baran, "Gradient based centralized optimal Volt/Var control strategy for smart distribution system," in *IEEE PES Innovative Smart Grid Technologies (ISGT)*, 2013.
- [9] K. Turitsyn, P. Sulc, S. Backhaus, and M. Chertkov, "Distributed control of reactive power flow in a radial distribution circuit with high photovoltaic penetration," in *IEEE PES General Meeting*, 2010, pp. 1-6.
- [10] J. Seuss, M. J. Reno, M. Lave, R. J. Broderick, and S. Grijalva, "Multi-Objective Advanced Inverter Controls to Dispatch the Real and Reactive Power of Many Distributed PV Systems," Sandia National Laboratories SAND2016-0023, 2016.
- [11] M. Oshiro, K. Tanaka, T. Senju, S. Toma, A. Yona, A. Y. Saber, et al., "Optimal voltage control in distribution systems using PV generators," *International Journal of Electrical Power & Energy Systems*, 2011.
- [12] Y. Chistyakov, E. Kholodova, K. Netreba, A. Szabo, and M. Metzger, "Combined central and local control of reactive power in electrical grids with distributed generation," in *IEEE International Energy Conference and Exhibition (ENERGYCON)*, 2012, pp. 325-330.
- [13] R. Caldon, M. Coppo, and R. Turri, "Distributed voltage control strategy for LV networks with inverter-interfaced generators," *Electric Power Systems Research*, vol. 107, pp. 85-92, 2/2014.
- [14] R. J. Broderick, J. E. Quiroz, M. J. Reno, A. Ellis, J. Smith, and R. Dugan, "Time Series Power Flow Analysis for Distribution Connected PV Generation," Sandia National Laboratories SAND2013-0537, 2013.
- [15] International Electrotechnical Commission (IEC), TR 61850-90-7, Object models for power converters in distributed energy resources (DER) systems, February 2013
- [16] J. E. Quiroz, M. J. Reno, and R. J. Broderick, "Time Series Simulation of Voltage Regulation Device Control Modes," in *IEEE Photovoltaic Specialists Conference*, 2013.
- [17] M. J. Reno and K. Coogan, "Grid Integrated Distributed PV (GridPV) Version 2," Sandia National Labs SAND2014-20141, 2014.
- [18] M. J. Reno, K. Coogan, R. J. Broderick, and S. Grijalva, "Reduction of Distribution Feeders for Simplified PV Impact Studies," in *IEEE Photovoltaic Specialists Conference*, 2013.
- [19] M. Lave, W. Hayes, A. Pohl, and C. W. Hansen, "Evaluation of Global Horizontal Irradiance to Plane-of-Array Irradiance Models at Locations Across the United States," *IEEE Journal of Photovoltaics*, vol. 5, 2015.
- [20] D. L. King, J. A. Kratochvil, and W. E. Boyson, "Photovoltaic array performance model," Sandia National Laboratories SAND2004-3535, 2004.
- [21] D. L. King, S. Gonzalez, G. M. Galbraith, and W. E. Boyson, "Performance model for grid-connected photovoltaic inverters," Sandia National Laboratories SAND2007-5036, 2007.
- [22] A. Samadi, R. Eriksson, L. Soder, B. G. Rawl, and J. C. Boemer, "Coordinated Active Power-Dependent Voltage Regulation in Distribution Grids With PV Systems," *IEEE Transactions on Power Delivery*, vol. 29, 2014.
- [23] S. Gonzalez, J. Johnson, M. J. Reno, and T. Zgonena, "Small Commercial Inverter Laboratory Evaluations of UL 1741 SA Grid-Support Function Response Times," in *IEEE Photovoltaic Specialists Conference (PVSC)*, 2016.
- [24] M. J. Reno, M. Lave, J. E. Quiroz, and R. J. Broderick, "PV Ramp Rate Smoothing Using Energy Storage to Mitigate Increased Voltage Regulator Tapping," in *IEEE Photovoltaic Specialists Conference*, 2016.
- [25] Standard C84.1-2011 American National Standard For Electric Power Systems and Equipment - Voltage Ratings (60 Hz),

Sandia National Laboratories is a multi-program laboratory managed and operated by Sandia Corporation, a wholly owned subsidiary of Lockheed Martin Corporation, for the U.S. Department of Energy's National Nuclear Security Administration under contract DE-AC04-94AL85000.